

Effect of stress anisotropy on hysteresis and Barkhausen noise in amorphous materials

C. Appino, G. Durin, V. Basso, C. Beatrice, M. Pasquale,^{a)} and G. Bertotti
 IEN Galileo Ferraris and INFN, C.so M. D'Azeglio 42, 10125 Torino, Italy

Hysteresis, power losses, and the Barkhausen effect are investigated in an Fe-based highly magnetostrictive amorphous material, as a function of applied stress. By means of the static and dynamic Preisach model, and of existing theories of the Barkhausen effect, the results are shown to be compatible with the existence of a characteristic structural length δ_c , playing a role similar to that of grain size in crystalline materials. At low applied stresses, where the magnetization process is dominated by quenched-in stresses σ_i , δ_c is identified with the typical wavelength of σ_i fluctuations. The theoretical analysis leads to the estimate $\delta_c \sim 70\text{--}100\ \mu\text{m}$ and $\langle \sigma_i \rangle \sim 3.5\ \text{MPa}$.
 © 1999 American Institute of Physics. [S0021-8979(99)24308-3]

I. INTRODUCTION

Knowledge of the microstructure of a magnetic material is the starting point for the prediction of hysteresis loop shapes and power losses. At the same time, the study of these magnetic properties can give valuable information about microstructural features. In polycrystalline soft magnetic materials, the average grain size $\langle s \rangle$ is often found to be the suitable parameter to summarize the influence of the microstructure. For instance, in rapidly quenched Si-Fe ribbons with different magnetostriction values, the hysteresis losses W_h follow the simple law $W_h = W_{h0} + c/\langle s \rangle$, with $\langle s \rangle$ spanning over one order of magnitude.¹ In addition, the behavior of the excess losses W_{exc} vs $\langle s \rangle$ points to the existence of characteristic correlation regions controlling the magnetization reversal under dynamic conditions, with linear size approximately equal to $\langle s \rangle$.

A similar characteristic correlation length δ_c in amorphous and nanocrystalline materials is less easily identifiable, as long as microstructural features control it. Amorphous alloys with high² or low³ magnetostriction show similar dependence of W_h on the longitudinal anisotropy K_u , induced either by applied stress or through annealing under a longitudinal saturating field. This at least suggests the existence of a common parameter governing the loss behavior. Following these results, in this article we investigate magnetization processes, hysteresis, and losses in the high-magnetostriction ($\lambda_s = 46.5 \times 10^{-6}$) $\text{Fe}_{64}\text{Co}_{21}\text{B}_{15}$ amorphous alloy. The high value of λ_s makes the applied stress σ an effective tool for inducing uniaxial anisotropies, obtaining radical changes of the domain structure and, consequently, of the hysteresis loop shape and loss figure. As usual in such magnetostrictive amorphous materials,² W_h has a characteristic dependence on σ , with a rapid decrease up to some characteristic value $\sigma_0 = 10\ \text{MPa}$ (region I), and then a slight increase under larger stresses (region II) (Fig. 1). The hysteresis and loss properties in both regions are investigated through the static and dynamic Preisach model,⁴ and combined with Barkhausen effect studies. In the region I, a cor-

relation length δ_c can be clearly identified, of the order of the wavelength of fluctuating stresses σ_i frozen-in during quenching.⁵ Remarkably, this single parameter δ_c controls, through the dynamic Preisach model, the entire phenomenology under dynamic excitation, i.e., the shape of dynamic hysteresis loops as a function of peak induction and magnetization frequency. In addition, from the reversible susceptibility at high fields,⁶ the average intensity of frozen-in stresses $\langle \sigma_i \rangle$ could also be obtained.⁵ In region II, the effect of σ_i on hysteresis and losses becomes negligible, as long as the magnetization processes is dominated by the induced long-range anisotropy.

II. EXPERIMENTAL RESULTS AND DATA ANALYSIS

Amorphous ribbons with composition $\text{Fe}_{64}\text{Co}_{21}\text{B}_{15}$ were produced by planar flow casting in air (width $w = 10\ \text{mm}$, thickness $d = 25\ \mu\text{m}$). Single strips of length $L = 300\ \text{mm}$ are

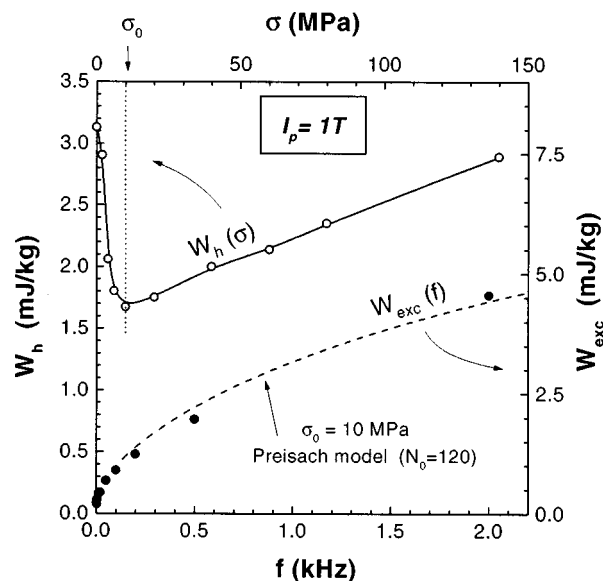


FIG. 1. Hysteresis losses per cycle at peak induction of 1 T at different stresses (top left) and the excess loss per cycle at $\sigma_0 = 10\ \text{MPa}$ (bottom right). The dynamical Preisach model prediction ($N_0 = 120$, dash line) and the experimental data nearly follow \sqrt{f} .

^{a)}Electronic mail: pasquale@ien.it

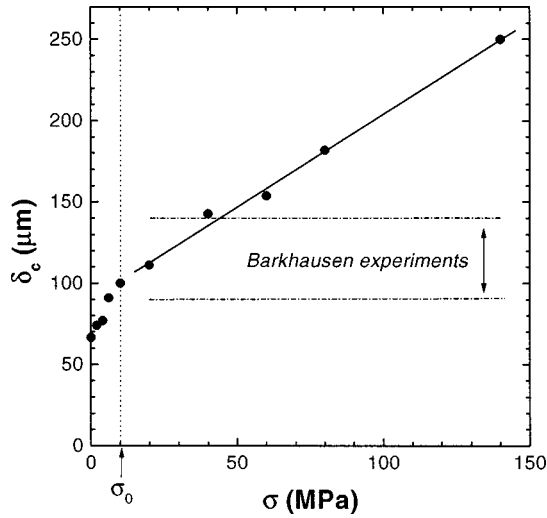


FIG. 2. The wavelength δ_c of the spatial correlation as a function of applied stress estimated from the dynamical Preisach model (symbols) and from the cutoff S_0 of the distributions of Barkhausen jump size ($\delta_c \sim S_0/2I_s d$).

measured under a tensile applied stress σ up to 140 MPa. For each stress value, a set of 20 quasi-static symmetric loops of increasing amplitude from zero to saturation are measured to get the Preisach distributions,⁷ assumed to have the form $p(h_c, h_u) = p_{\text{irr}}(h_c, h_u) + \delta(h_c)p_{\text{rev}}(h_u)$ where p_{irr} and p_{rev} give information on the various irreversible and reversible magnetization processes. Dynamic hysteresis loops and power losses are measured under controlled sinusoidal flux conditions, in the frequency range of $f = 2 \text{ Hz} - 10 \text{ kHz}$, at the peak inductions of $I_p = 1 \text{ T}$ and $I_p = 1.3 \text{ T}$. Loss separation analysis is carried out to obtain the hysteresis loss W_h and the excess loss W_{exc} . The latter was found to be nearly proportional to \sqrt{f} up to frequencies of the order of 1–2 kHz (Fig. 1). At larger frequencies, deviations from the square-root law are observed, particularly at large stresses.

Knowledge of the Preisach distribution $p(h_c, h_u)$ together with the assumption of the number N_0 of correlation regions providing coherent magnetization reversal, permits the dynamic hysteresis loops and losses to be predicted. For each stress, the best value of N_0 matching measured and calculated loop shapes is found. An example of the calculated excess loss is shown in Fig. 1 (broken line). Assuming columnar correlation regions spanning the entire ribbon thickness w , the correlation lengths are simply estimated as $\delta_c = w/N_0$, and found to linearly increase for $\sigma > \sigma_0$ (Fig. 2).

Finally, Barkhausen effect measurements are performed⁸ to study the distribution of the size S and duration T of the Barkhausen jumps occurring in the central part of the saturation hysteresis loop, as a function of σ . The measured distributions have the form $P(S) \sim S^{-\tau} f(S/S_0)$, $P(T) \sim T^{-\alpha} g(T/T_0)$, with $\tau \sim 1.28$ and $\alpha \sim 1.5$, both independent of the stress, provided that $\sigma > \sigma_0$. Data in region I are more affected by the background noise, and no definitive evaluations of the results can be made. The values of these scaling exponents are compared with the predictions of existing theories,⁹ to extract information on the domain wall behavior during magnetization reversal. In particular, such values are found to be related to a domain wall motion totally domi-

nated only by the surface tension of the wall, and not by local magnetic charges arising from local perturbations of the domain wall. This is in agreement with the change in the domain structure induced by stress. In addition, the cutoff size S_0 is analyzed as a function of σ and compared with δ_c (Fig. 2). In fact, S_0 represents the maximum size of an individual Barkhausen jump, and this size is expected to be limited by the structural inhomogeneities described by δ_c .

III. DISCUSSION AND CONCLUSIONS

In a picture where randomly distributed quenched-in stresses represent the dominant microstructural feature, two parameters are expected to be relevant: the typical quenched-in stress intensity $\langle \sigma_i \rangle$ and the typical wavelength δ_c of spatial correlation. The former can be estimated using the static Preisach distribution component $p_{\text{rev}}(h_u)$ which describes reversible magnetization processes, due to the motion of domain walls around a metastable position, and coherent rotation of the magnetization against random local anisotropies. The rotation process is expected to dominate at large magnetic fields, and should be directly connected to the high field shape of the p_{rev} distribution. A quantitative evaluation of this connection is obtained using the model developed in Ref. 6. Here a set of independent mesoscopic regions can be characterized by a uniaxial random anisotropy K due to quenched-in stresses, superposed to the long-range anisotropy K_u induced by the applied stress σ . By minimizing the sum of the anisotropy energy and the energy of interaction with the applied field, averaged over a suitable distribution of local anisotropies, the reversible susceptibility can be written as $\chi_{\text{rev}}(H) = (0.79 I_{s,\text{rev}}/H_0) \exp[-(H/H_0)^{0.7}]$, where $H_0 = \langle K \rangle / 2I_s$ is a characteristic field proportional to the average intensity $\langle K \rangle$ of quenched-in anisotropies, and $I_{s,\text{rev}}$ is the total reversible magnetization. In the Preisach approach, $\chi_{\text{rev}}(H) = 2p_{\text{rev}}(H)$, so that a quantitative comparison of the two predictions can be made (Fig. 3). The tails of both distributions are described very well at different stresses keeping $\langle K \rangle = 250 \text{ J/m}^3$ fixed. According to the model of Ref. 6, the drastic reduction of $I_{s,\text{rev}}$ with σ is also expected. As shown by the inset of Fig. 3, this theoretical prediction deviates from the reconstructed p_{rev} at low fields, due to the fact that reversible domain wall motion contributes to p_{rev} in this region, which is not taken into account by the model.

In region I ($\sigma < \sigma_0$), maze domain structures with complex topology are present and coercivity is dominated by the distribution of internal stresses σ_i . Conversely, simple structures of bar-like longitudinal domains are set in region II ($\sigma > \sigma_0$), as the anisotropy induced by the applied stress has become definitely larger than quenched-in anisotropies. The stress σ_0 therefore overcomes most of the internal stresses, and should be equal to a few times $\langle \sigma_i \rangle$, in agreement with the estimation $\langle \sigma_i \rangle \approx (2/3) \langle K \rangle / \lambda_s \sim 3.5 \text{ MPa}$, giving $\sigma_0 \sim 3 \langle \sigma_i \rangle$.

The wavelength δ_c of spatial correlation of quenched-in stress is estimated using the irreversible Preisach component and the Barkhausen distribution of jump sizes.

The Preisach component $p_{\text{irr}}(h_c, h_u)$ contains information on the switching field distribution of dissipative pro-

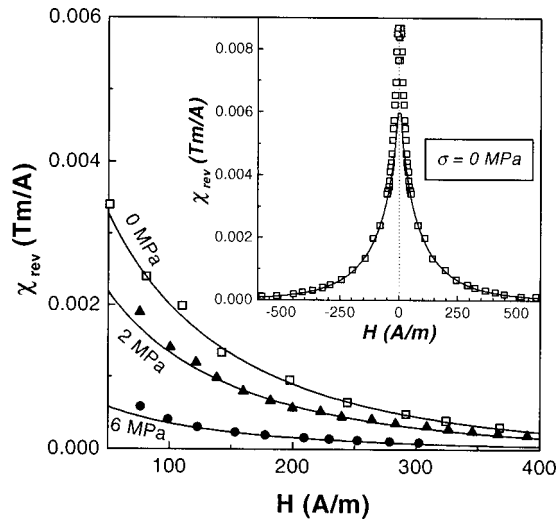


FIG. 3. Reversible susceptibility $\chi_{\text{rev}}(H) = 2p_{\text{rev}}(H)$ obtained from the reconstructed Preisach distributions (symbols) at different stresses compared (continuous lines) to the model of Ref. 6 giving $\chi_{\text{rev}}(H) = (0.79I_{s,\text{rev}}/H_0)\exp[-(H/H_0)^{0.7}]$, where $H_0 = \langle K \rangle / 2I_s$, with $H_0 = 72$ A/m, $\langle K \rangle = 250$ J/m³, $I_s = 1.75$ T, and $I_{s,\text{rev}} = 0.45$ T (0 MPa), 0.30 (2 MPa), 0.08 (6 MPa). (Inset) Data at $\sigma = 0$ MPa in the full range of the applied field.

cesses, typically, domain wall Barkhausen jumps. A convenient representation is obtained by considering the integrated distribution $p(h_c) = \int p_{\text{irr}}(h_c, h_u) dh_r$, which can be interpreted as the distribution of local coercive fields experienced by the domain structure. We find that $p(h_c)$ is described by the lognormal distribution $\exp[-\ln^2(h_c/\langle h_c \rangle)/2\Delta_c^2]/h_c$, with a mean value $\langle h_c \rangle$ decreasing from 10 to 5 A/m, and a variance Δ_c decreasing 0.7 to 0.4 A/m only in region I, and nearly independent of the stress in region II. On passing from

low to high σ , the regions with higher coercivity are progressively eliminated and $p(h_c)$ becomes sharply peaked around $h_c \cong 4-5$ A/m. These hard regions are probably associated with the complex domain pattern of the unstressed state, and progressively destroyed by the onset of the long-range anisotropy induced by the stress.

The distributions $p(h_c)$ are used to estimate the dependence of δ_c on σ , shown in Fig. 2. In region I, where internal stresses dominate, $\delta_c \sim 70-100$ μm , in agreement with the estimate of domain size and wavelength of quenched-in stresses given in Ref. 5. In region II, the increase of δ_c is related to increase of the size of bar-like domains.

A similar estimation of δ_c is obtained from the cutoff S_0 of the Barkhausen size distributions, which is related to the largest domain wall displacement during a jump. In fact, we expect this displacement to be of the order of the correlation region described by δ_c . As $S_0 = 2I_s d \delta_c \sim 0.8-1.2 \times 10^{-8}$ Wb, we get $\delta_c \sim 90-140$ μm (Fig. 3), in reasonable agreement with the estimation above.

- ¹C. Appino, E. Ferrara, F. Fiorillo, I. Suberbielle, J. Degauque, C. Lebourg, and M. Baricco, *J. Phys. IV* **8**, 531 (1998).
- ²G. Bertotti, E. Ferrara, F. Fiorillo, and P. Tiberto, *Mater. Sci. Eng., A* **226-228**, 603 (1997).
- ³C. Beatrice, C. Appino, E. Ferrara, and F. Fiorillo, *J. Magn. Magn. Mater.* **160**, 302 (1996).
- ⁴G. Bertotti, *IEEE Trans. Magn.* **28**, 2599 (1992).
- ⁵H. Kronmüller, *Atomic Energy Rev. Internat. Atom. En. Agency (Vienne)* **1**, 255 (1981).
- ⁶C. Appino and F. Fiorillo, *J. Appl. Phys.* **76**, 5371 (1994).
- ⁷V. Basso, G. Bertotti, A. Infortuna, and M. Pasquale, *IEEE Trans. Magn.* **31**, 4000 (1995).
- ⁸G. Durin and S. Zapperi, *J. Appl. Phys.* (these proceedings).
- ⁹P. Cizeau, S. Zapperi, G. Durin, and H.E. Stanley, *Phys. Rev. Lett.* **79**, 4669 (1997); S. Zapperi, P. Cizeau, G. Durin, and H.E. Stanley, *Phys. Rev. B* **58**, 6353 (1998).